Available online at www.sciencedirect.com
SCIENCE DIRECT
Journal of Molecular Graphics and Modelling 24 (2005) 102–110
Journal of Molecular Graphics and Modelling
www.elsevier.com/locate/JMGM

An implementation of the nudged elastic band algorithm and application to the reaction mechanism of HGXPRTase from *Plasmodium falciparum*

Ramon Crehuet [a,*], Aline Thomas [b], Martin J. Field [b,**]

[a] *Institut d'Investigacions Químiques i Ambientals de Barcelona (CSIC), Jordi Girona 18–26, 08034 Barcelona, Spain*
[b] *Laboratoire de Dynamique Moléculaire, Institut de Biologie Structurale (CEA–CNRS), 41 rue Jules Horowitz, 38027 Grenoble Cedex 1, France*

Accepted 20 April 2005
Available online 13 June 2005

Abstract

The understanding of transition processes, such as chemical reactions, is a central topic in theoretical molecular science. A common approach for investigating such processes is to calculate paths between reactant and product structures that are representative of the transition. Many approaches have been proposed to determine such paths but, in this paper, we examine the nudged elastic band algorithm which was recently introduced by Jónsson and co-workers and has been used to study a wide range of transition problems. We describe our implementation of the method in the simulation program DYNAMO and some modifications to the original algorithm that we found improve its efficiency. The use of the method is illustrated by an application to the reaction mechanism of the enzyme hypoxanthine-guanine-xanthine phosphoribosyltransferase from *Plasmodium falciparum*.

Keywords: DYNAMO program; Enzymatic reactions; Hybrid QM/MM potentials; Nudged elastic band algorithm; Reaction paths

1. Introduction

The chemical and physical behaviour of a molecule depends entirely on the shape of its potential energy surface (PES). Because of the high dimensionality of this surface, a complete exploration is and will continue to be unfeasible except for the smallest molecules. Methods and theories that rely on a subset of the PES have been developed since the 1930s when Eyring presented the foundations of transition state theory [1]. Since then the traditional way of investigating a reaction mechanism theoretically has been to locate transition states (TSs) and to follow downhill the steepest descent directions that lead to the adjacent minima. This procedure maps out the minimum energy path (MEP) for a transition process that connects reactants and products (see [2] for a review). Although powerful, this approach has some drawbacks. First, effective TS (or saddle point) location algorithms require the second coordinate derivatives of the potential energy surface. These are prohibitively expensive to calculate and to manipulate for large systems. Second, most algorithms require a good starting guess for the TS structure which, in practice, means that a particular reaction mechanism must be assumed.

Chain-of-states methods tackle these problems by finding MEPs given only initial and final structures – for example, those of reactants and products – and by employing algorithms that require first derivatives only. In these methods a reaction path is represented as a set of N structures that go from the initial to final states and then the set of structures is concertedly optimized toward the MEP. An early algorithm of this type was formulated by Czerminski and Elber [3] but this had several shortcomings [4–6]. An improved and more robust algorithm, the nudged elastic band (NEB) method, was introduced by Jónsson and co-workers and this has been widely applied in many different contexts [5,4].

The methods described so far find paths on the PES and thus do not account for dynamical and entropic effects. In

* Corresponding author. Tel.: +34 934006111.
** Corresponding author.
E-mail addresses: rcsqtc@iiqab.csic.es (R. Crehuet), athomas@ibs.fr (A. Thomas), mjfield@ibs.fr (M.J. Field).

1093-3263/$ – see front matter © 2005 Elsevier Inc. All rights reserved.
doi:10.1016/j.jmgm.2005.05.003

studying condensed phase reactions it is usually preferable to consider free energies, instead of potential energies, but the calculation of reaction free energies can be very expensive. Many methods exist [7,8] but most of them determine free energies as functions of a single or a very small number of variables that define the reaction process. A proper choice of such variables is crucial, especially at the TS region, because the wrong choice of variables can mean sampling configurations of the system that do not belong to the TS dividing surface and lead to free-energy barriers that are incorrect. In contrast, the NEB method does not require the specification of any privileged variables and so it can help in the choice or the verification of the variables for a free-energy calculation. Likewise a NEB path could itself serve as the reaction coordinate for the calculation of a free-energy profile as has been done for MEPs determined by other algorithms (see, for example, Ref. [9]).

The aim of this article is two-fold. First of all, we describe our implementation of the NEB algorithm and some modifications to the original algorithm that we found improve efficiency. Second, we illustrate the NEB method with application to an enzyme reaction. We have chosen the protein hypoxanthine–guanine–xanthine phosphoribosyltransferase (HGXPRTase) because this is a protein that we have studied extensively before with other theoretical methods [10]. HGXPRTase is from the protozoan parasite *Plasmodium falciparum* which is the causative agent of malaria. It is an essential enzyme as it forms part of the pathway that scavenges purine bases from the parasite's host (see Refs. [11] and [12] for reviews). It is of interest because the equivalent human enzyme shows a much reduced affinity for xanthine, a difference which could be crucial for the design of selective inhibitors and, hence, of antimalarial agents.

All our work was done in the DYNAMO program [7,13] which is a library of Fortran 90/95 subroutines designed for performing simulations of biomolecular systems with hybrid quantum mechanical (QM)/molecular mechanical (MM) potentials [14,15]. These QM/MM methods are particularly well adapted for investigating reactions in large condensed phase systems, such as enzymes.

The outline of this paper is as follows. Section 2 describes the details of our simulation systems and the original NEB method, Section 3 describes the modifications that we have made to the NEB algorithm and Section 4 the results we obtained for the enzyme reaction mechanism. Section 5 concludes.

2. Methods

2.1. Blocked alanine

The principal system of study in this paper is the HGXPRTase enzyme but simpler tests were done on a smaller system, blocked alanine (bALA), which is also known as the alanine dipeptide. Although bALA is a relatively simple molecule, it is far more complex than the two-dimensional surfaces that are often used in testing chain-of-states methods. bALA has been used extensively by other workers (see, for example, Refs. [16,17]) because it has enough complexity to show several minima and reaction paths. We focused on the transition between the C_{7eq} and C_{ax} conformers (Fig. 1). The system was described with the OPLS all-atom force field [18] and no solvent was included.

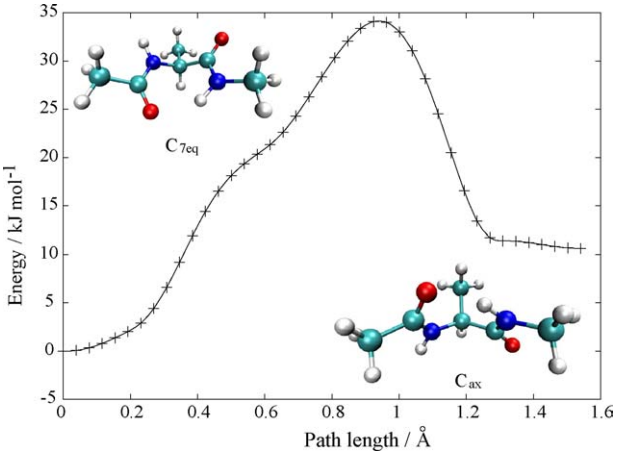

Fig. 1. Reactant and product structures and the NEB energy profile for the C_{7eq} to C_{ax} transition in blocked alanine.

2.2. HGXPRTase

The reaction mechanism of the HGXPRTase enzyme is one we have already studied extensively using both traditional, second derivative, TS-location algorithms and free-energy calculations [10]. Because we wanted to compare the results given by NEB with our previous work, the simulation system was the same as the one we used before. A brief description of the system is given here but full details may be found in Ref. [10]. A schematic of the reaction catalyzed by the enzyme is given in Fig. 2.

2.2.1. The enzyme model

The coordinates of the enzyme were taken from the 2.0 Å resolution crystal structure, 1CJB, of the protein data bank [19] which was co-crystallized with a TS-analogue inhibitor. The higher resolution structure 1FSG [20] was also used to model the phosphoribosyl-pyrophosphate (PRPP) moiety in the active site because in this structure the optimized substrates fitted better the crystal structure. The enzyme was solvated in a cubic box of water of side 70 Å and thermalized at 300 K. The final system included 129 and 6480 water molecules from the crystal structure and the water box, respectively.

2.2.2. Hybrid potential simulations

All the QM/MM simulations were performed with the DYNAMO library [7,13]. The system was partitioned into a QM and a MM region. The QM region was treated with the

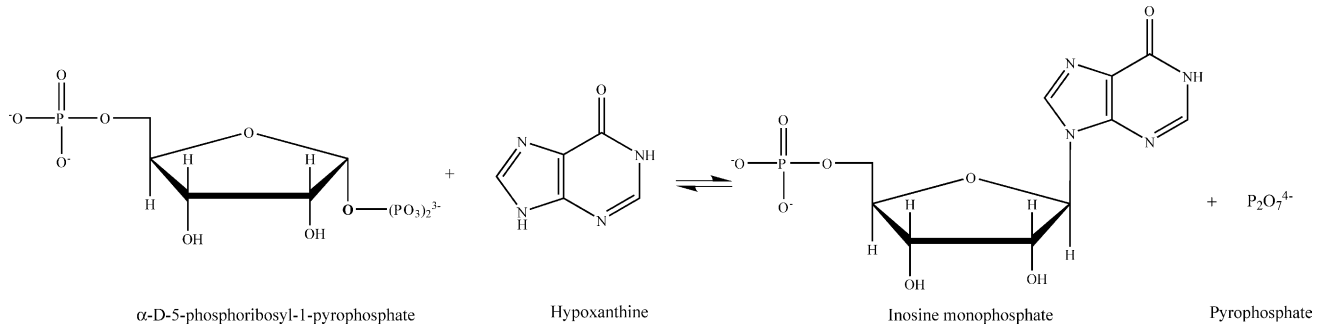

Fig. 2. The reaction catalyzed by HGXPRTase.

AM1 Hamiltonian [21] and included the substrates (PRPP and hypoxanthine), the two magnesium ions and their coordinating ligands, including five waters and Asp204, and the catalytic residue Asp148, giving 75 QM atoms in total. The remainder of the system was treated with the OPLS all-atom force field [18]. The covalent bonds between the QM and the MM regions were treated with the link-atom methodology [13]. The complete system contained 23,533 atoms. Of these, only 979 were free to move in the NEB calculations, the other 22,554 being fixed. The choice of atoms to move was made by selecting all those within a sphere of 11 Å radius centred on the C1′ atom of the ribose cycle in PRPP. Non-covalent interactions were truncated with an atom-based force-switching approximation with a 8.0 Å inner cutoff and a 12.0 Å outer cutoff.

2.3. The NEB method

The NEB method is based on the discretization of the path into a set of N structures. Initial and final structures represent reactants and prducts and are held fixed. The remaining $N-2$ structures are optimized towards the MEP by displacing each structure downhill along the gradient vector. To keep structures equally spaced, harmonic potentials or spring forces connect each structure with its two neighbours. The forces felt by a structure i in the NEB are defined to consist of two components — one perpendicular to the tangent of the path that originates from the gradient of the PES and another parallel to the path created by the springs. These forces may be written:

$$\mathbf{F}_i^{\parallel} = k(|\mathbf{R}_{i+1} - \mathbf{R}_i| - |\mathbf{R}_i - \mathbf{R}_{i-1}|)\hat{\boldsymbol{\tau}}_i,$$
$$\mathbf{F}_i^{\perp} = \mathbf{g}_i^{\perp} = \mathbf{g}_i - \mathbf{g}_i \cdot \hat{\boldsymbol{\tau}}_i \hat{\boldsymbol{\tau}}_i \quad (1)$$

where k is the spring force constant, $\mathbf{R}_i$ the coordinate vector for structure i, $\hat{\boldsymbol{\tau}}_i$ the normalized tangent to the path and $\mathbf{g}_i$ is the force due to the potential energy function.

The projection of the forces in this way renders them non-conservative, making traditional minimization methods difficult to apply for a NEB optimization. We have adopted the approach employed by Jónsson and co-workers in which the forces are quenched following a damped velocity Verlet algorithm. This is a traditional Verlet algorithm (see, for example, Ref. [7]) but in which the velocity is projected onto the force at each step, and is zeroed when the projection has a negative sign. For further details of the original algorithm, see Ref. [5]. Recently a number of variations to the NEB have been published that use more efficient optimization methods [22–24]. A comparison of our method with these other methods would be interesting and will be considered in future work.

For a discretized path, such as a NEB, the correct definition of the tangent vector, $\boldsymbol{\tau}$, is crucial. Henkelman and Jónsson found that their initial definition led to instabilities [25] and they derived a new definition. We have adopted their new tangent but have reformulated it as a simpler expression, avoiding the use of absolute values (c.f. Eqs. (8) and (10) of Ref. [25]):

$$\boldsymbol{\tau}_i = \begin{cases} \boldsymbol{\tau}_i^+ & \text{if } V_{i+1} > V_i > V_{i-1} \\ \boldsymbol{\tau}_i^- & \text{if } V_{i+1} < V_i < V_{i-1} \\ \boldsymbol{\tau}_i^+(V_i - V_{i-1}) + \boldsymbol{\tau}_i^-(V_i - V_{i+1}) & \text{if } V_{i+1} < V_i > V_{i-1} \\ \boldsymbol{\tau}_i^+(V_{i+1} - V_i) + \boldsymbol{\tau}_i^-(V_{i-1} - V_i) & \text{if } V_{i+1} > V_i < V_{i-1} \end{cases} \quad (2)$$

where $\boldsymbol{\tau}_i^+ = \mathbf{R}_{i+1} - \mathbf{R}_i$ and $\boldsymbol{\tau}_i^- = \mathbf{R}_i - \mathbf{R}_{i-1}$. Note that the tangent vectors have to be normalized for use in Eq. (1).

3. Modifications to the original NEB algorithm

The NEB minimization involves the calculation of the gradient for each structure in the chain. The optimization of a structure is relatively decoupled from that of its neighbours as the spring forces serve to keep the structures equally separated and so restrain only a small number of degrees of freedom. This means that the optimization of a NEB with N points takes roughly twice the time of a NEB with $N/2$ points. Recently a NEB method with a variable number of points has been suggested in Ref. [26]. We found that a simpler strategy was also satisfactory and could account for those paths that had multiple minima. The strategy consists in starting with a small number of points, usually 7 or 9. If we see that the final NEB seems to contain more than one barrier, each point close to a valley is minimized and the

NEB is split into different chains containing just one TS. Then the number of points is increased and reoptimized until the energy profile does not vary appreciably. Because the length of the paths may be very different for different mechanisms, the number of points needed to get a good resolution is also variable. If one wants a higher resolution of the barrier, one does not need to optimize a NEB connecting two minima, instead, one can zoom in on the barrier region. Our experience indicates that as long as the first and last points have lower energy than their neighbours, the optimization of the NEB will run smoothly. This scheme is similar to the automatic one described in Ref. [27].

Liu and co-workers recently published a work on the use of NEB to study enzymatic reactions [28]. They added a modification to the original NEB that can be summarized as follows. They separate the enzyme's degrees of freedom into an active and a passive group. The passive or spectator coordinates are not considered when calculating the interpoint distance, so that they can move freely and be always minimized. The advantage is that one can have a better resolution of the active degrees of freedom along the NEB. Unfortunately, this assumes that any conformational change on the passive degrees of freedom is orthogonal to the transition vector, or, in other words, that this conformational change does not contribute to the energy barrier. Because of this, and because the reaction in HGXPRTase does not involve large conformational changes, we think this modification is not necessary in this study. We emphasise that each point in the NEB chain is a full replica of the whole enzyme system, with the same number of QM, MM, fixed and free atoms. Therefore the distance between the NEB points corresponds to movements of all the 979 free atoms, which, in principle, can all contribute to the energy barrier. The authors in [28] also address the problem of uneven point spacing for complex systems but we believe that splitting the NEB for each step in a reaction mechanism as explained above and using the corrected tangent described by Henkelman and Jónsson [25] gives satisfactory results.

We have previously stated that the NEB method does not assume a predefined reaction mechanism. This is not entirely true. It would be so if we could do a 'global' optimization of the NEB, but global optimizations are, in general, daunting tasks and all methods and variants of the NEB perform local optimizations. In such cases, the initial chain becomes relevant as the NEB method will optimize to the MEP closest to the initial guess. Because of this, we recommend optimizing from as many different starting pairs of initial and final structures as possible. The simplest guess, and the one that most implementations of NEB seem to use, is a chain of structures linearly interpolated from the starting and ending structures. This is equivalent to assuming a concerted mechanism. When stepwise mechanisms may be possible, we recommend constructing structures for possible intermediates or TSs along the pathway and then optimizing NEBs between each of the intermediate structures first before piecing them together and performing an optimization on the combined path. The guess structures need only be crude as they will eventually be optimized during the NEB process. To facilitate the creation of starting guesses for NEB optimization in this way, we have implemented a series of tools that permit the generation of intermediate structures and the manipulation of NEB pathways.

As we have explained, we have used the damped velocity Verlet algorithm introduced by Jónsson et al. [5] for NEB optimizations. This method is very robust but has slow convergence close to the minima as it is, in essence, a scaled, steepest-descent method. To improve the convergence speed we have introduced two changes and tested some other possibilities. The first modification concerns how to project the velocity vector. There are three possibilities: the complete velocity vector for the $N-2$ structures can be projected onto the complete force (full projection), the velocity for each structure can be projected independently (structure projection) or the velocity for each atom can be projected onto its force (atom projection). Fig. 3 shows an example of a NEB optimization using these three different methods. It is clear that atom projections are more efficient than the other two, which have similar behaviour.

The second modification concerns the number of points moved at each iteration. Because the path may have a complex shape, some points will reach the MEP faster than others. Thus, moving all $N-2$ points at each iteration may be unnecessary. Instead, we have devised a procedure in which only the point that has a higher force is moved. Moving one point implies that only one gradient needs to be calculated at each iteration but, according to Eq. (1), the forces on its neighbouring points can also change and have to be updated. Fig. 3 illustrates the reduction in the number of gradient evaluations that is possible when only one image is moved at a time (using the more efficient atom velocity

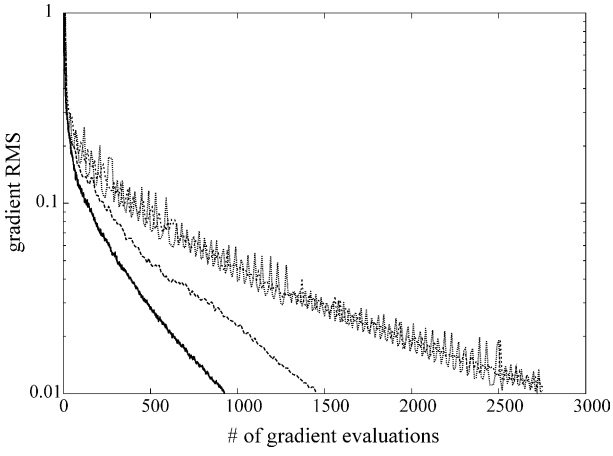

Fig. 3. Convergence rates for NEB optimizations using different velocity projection schemes. Full projection (dotted line) and structure projection (bold short-dashes) perform similarly. Atom projection (dashes) is better but is improved even more when a single structure per step is moved (solid). The calculations were done on the C_{7eq}–C_{ax} transition in blocked alanine. The root mean square (RMS) gradient is evaluated for the atoms of all the structures in the path and has units of kJ mol^{-1} Å^{-1}.

projection). This procedure becomes even better when a chain of N structures is expanded to one of $2N - 1$ structures by introducing new points between the existing ones. In such a case, only half of the points will have to be substantially optimized as the others will move only slightly.

We have considered two other modifications that did not work. First, a variable mass or equivalently a variable time step was tried. The aim was to be able to have larger time steps when forces are small close to the minima. Unfortunately the algorithm became unstable too easily. Second, a Newton–Rhapson scheme was implemented for the spring potential. As the spring force corresponds to a harmonic potential whose minimum can be calculated exactly for any given pair of points, one can take second order steps for the parallel force in Eq. (1). This scheme gave very good results when applied to the model Müller–Brown surface [29] but did not lead to improved performance for more complicated systems (data not shown). The reason is probably that the Müller-Brown surface is a bi-dimensional potential and, for each image, one degree of freedom comes from the potential and the other from the spring forces. In contrast, any reasonably large molecular system has a large number of degrees of freedom that will contribute to the perpendicular force, and still only one to the spring force. The minimization of the former becomes the bottleneck for the optimization and therefore, any improvement in the optimization of the spring force potential is negligible.

Finally, we make a few technical points about the use of NEB with quantum chemical methods. First of all, it is important to ensure that the quantum chemical calculations for each structure in the starting NEB converge to the proper electronic state (usually the ground state). Once this has been accomplished, the NEB optimization will normally proceed without problems. However, because most computational software, including DYNAMO, will use the previously calculated electronic wave-functions or densities as initial guesses for subsequent calculations, one could face a situation in which, say, the second point wave-function is used to calculate the initial guess for the 23rd point wave-function, which may have a very different geometry. Instead, we have found it desirable to save the wave-functions for each structure at each NEB iteration and then retrieve them as appropriate. Saving the wavefunctions in this way can require significant disk storage but it is highly recommended for systems where convergence problems are common, such as when transition metals are present.

4. The HGXPRTase reaction mechanism

HGXPRTase catalyses the transfer of the 5-phosphoribosyl group from α-D-5-phosphoribosyl-1-pyrophosphate to a nitrogen atom of the imidazole ring of the purines hypoxanthine, guanine or xanthine (Fig. 2). Originally there was some dispute about the mechanism of the enzyme because some experiments indicated a dissociative, S_N1-like mechanism and others, a mechanism with some degree of associative character. The consensus now seems to be an

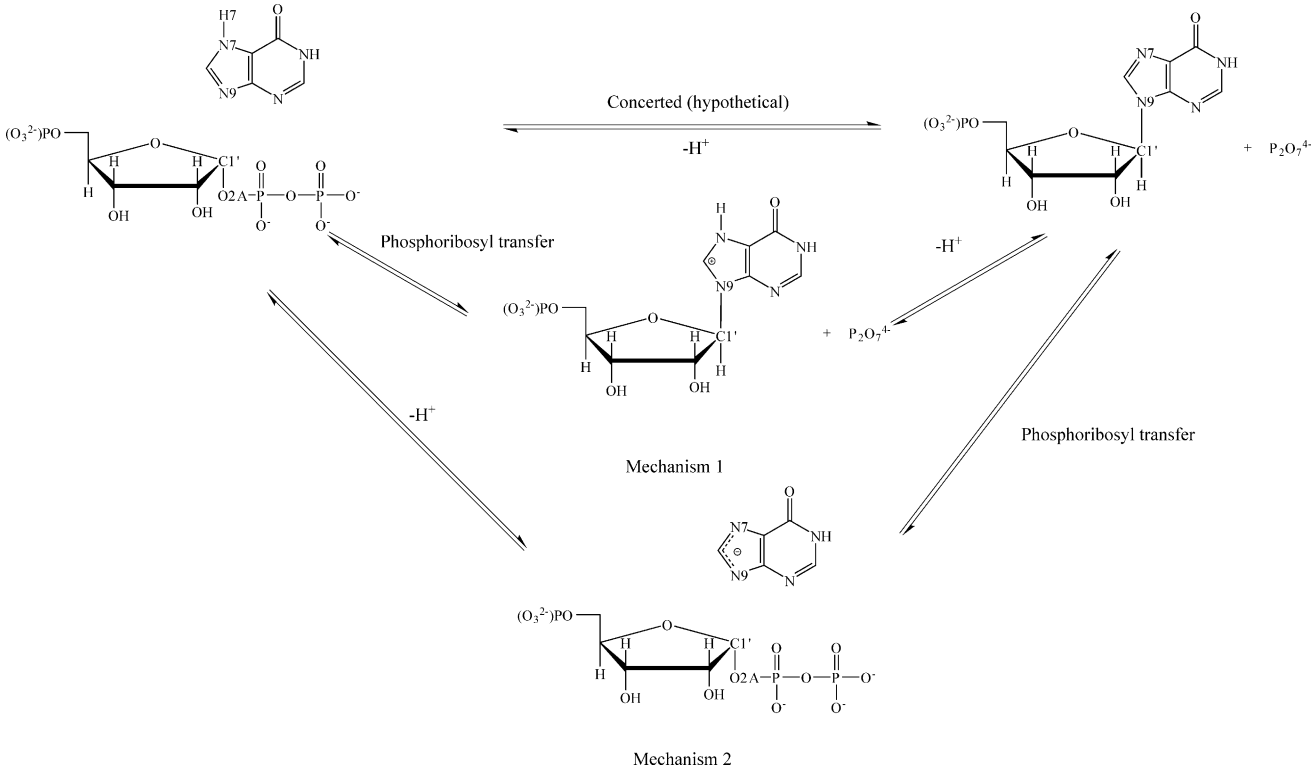

Fig. 4. Schemes of the reaction mechanisms of HGXPRTase discussed in the text. The atoms mentioned explicitly in the text are labelled.

associative mechanism of type D_NA_N (see Ref. [30] for a review), a result we also obtained in our previous work on this enzyme [10].

We investigated a number of possible mechanisms with the NEB method and the three that we discuss are shown in Fig. 4. There is a concerted mechanism that goes directly from reactants to products and two stepwise mechanisms, mechanisms 1 and 2. In mechanism 1, there is transfer of the phosphoribosyl group followed by a proton transfer from the hypoxanthine to an aspartic acid side-chain of the protein. In mechanism 2, the proton transfer occurs before the phosphoribosyl transfer.

The possibility of a concerted mechanism was quickly eliminated. Our previous free-energy calculations showed that the region of the free-energy surface corresponding to the concerted mechanism was of high energy but relatively flat so that a minimum in the PES might be possible. However, all our initial guesses corresponding to the concerted mechanism ended up as one of the stepwise mechanisms shown in Fig. 4.

In constrast, it was possible to find optimized NEB pathways for both stepwise mechanisms. Mechanism 1 has the nucleophilic attack before the proton transfer. From Fig. 5 it can be seen that this step has an energy profile with a pronounced shoulder. At the beginning of the shoulder, the C1′–O2A and C1′–N9 distances are 2.0 and 2.7 Å, respectively, whereas at the top of the barrier they are 2.0 and 2.8 Å, respectively. This high-energy region thus corresponds to attack by the hypoxanthine with little change in the ribosyl–pyrophosphate distance. The barrier for this step is 118 kJ mol^{-1}. The second step of a proton transfer has a barrier of only 7 kJ mol^{-1}. This barrier is so small because the reaction is highly exergonic (−90 kJ mol^{-1}) due to the stabilization that arises from the re-establishment of aromaticity in the hypoxanthine fragment.

The second mechanism starts with the proton transfer. Because aromaticity is already present in the reactant, the proton transfer has a higher energy barrier (39 kJ mol^{-1}) and is less exergonic (−34 kJ mol^{-1}) than in mechanism 1. The second step is more interesting. Here we find that the nucleophilic attack is in fact, composed of two steps, with a barely stable intermediate. In the first step, the C1′^{O2A} bond is cleaved and in the second the C1′^{N9} bond is formed. This corresponds to a S_N1 mechanism. Stated this way mechanisms 1 and 2 seem to differ considerably, but the difference between them is very subtle as there is only a tiny stabilization of the intermediate in mechanism 2 that does not exist in mechanism 1. It is possible, however, to identify two TSs. The first has C1′–N9 and C1′–O2A distances of 2.70 and 2.12 Å, respectively, and the second, C1′–N9 and C1′–O2A distances of 2.15 and 2.90 Å (see Fig. 6). The barrier for the second TS is the higher with a value of 100 kJ mol^{-1}. Mechanism 2 is also the one that we found to be favoured in our previous work although the free-energy barrier was lower and the plateau flatter without an obvious intermediate structure.

In both mechanisms 1 and 2, we see that the energy barrier is due to the nucleophilic substitution. In mechanism 1 this barrier is 118 kJ mol^{-1} and in mechanism 2 it is

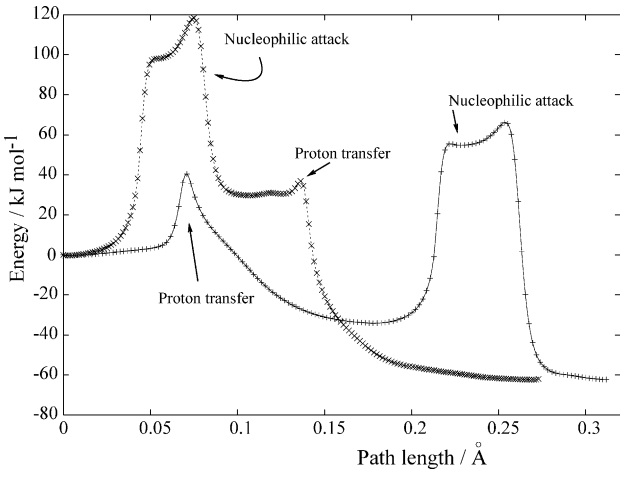

Fig. 5. Optimized NEB pathways for the stepwise mechanisms of the reaction catalyzed by HGXPRTase. Mechanism 1: diagonal crosses; mechanism 2: upright crosses.

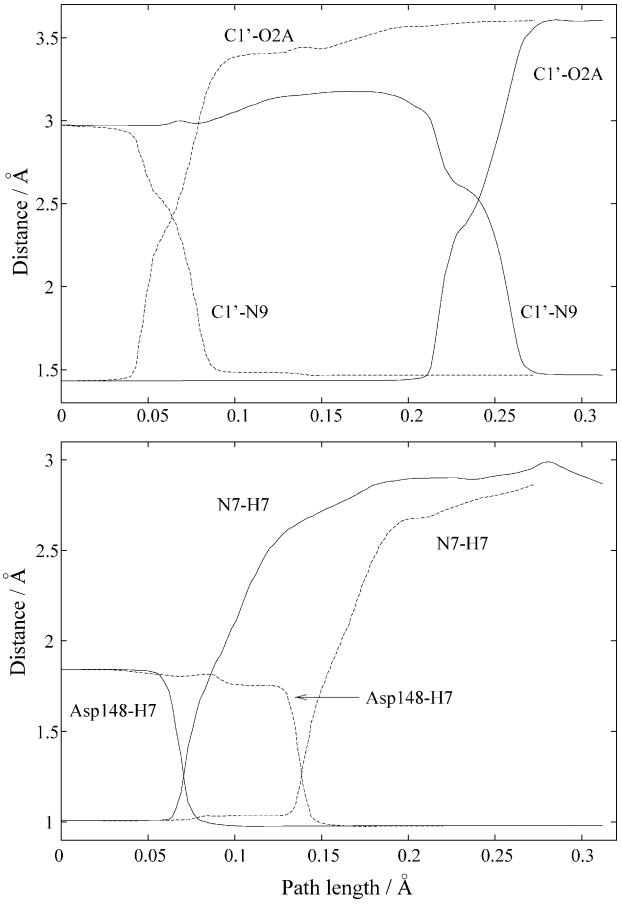

Fig. 6. Evolution of some relevant distances along the optimized NEB pathways for the phosphoribosyl transfer step (upper graph) and the proton transfer step (lower graph). Mechanism 1: dashed lines; mechanism 2: solid lines.

100 kJ mol^{-1}. This agrees with the Bell–Evans–Polanyi and Marcus principles that state that because this is a late TS it will resemble products, and because products are higher in energy (relative to reactants) for mechanism 1 than for mechanism 2, the barrier is higher for mechanism 1. Alternatively, one can say that a species with a negative charge, such as the hypoxanthine group of mechanism 2, is a better nucleophile than a neutral one.

As we have explained in the introduction, the NEB method gives a full reaction path and, thus, also a transition vector. We have analysed the transition vectors for both mechanisms and see that no degree of freedom contributes significantly to them apart from the C1′–O2A and C1′–N9 distances. This serves to validate the choice of variables that we used in our previous free-energy calculations. Fig. 7 shows the transition vector for mechanism 2.

4.1. Energy Contributions

As a further analysis of mechanism 2, we compare the energy contributions along the reaction path between the reaction in enzyme and in vacuum. This will not, of course, explain the catalytic effect of the enzyme, which should be compared to the reaction in water, but the results are interesting nonetheless. The choice of atoms to consider in the vacuum reaction is arbitrary but the results we present here are for the atoms of the QM region only. Note that we have not reoptimized the path in vacuum because we want to compare energy contributions for the same structures that occur in the enzyme.

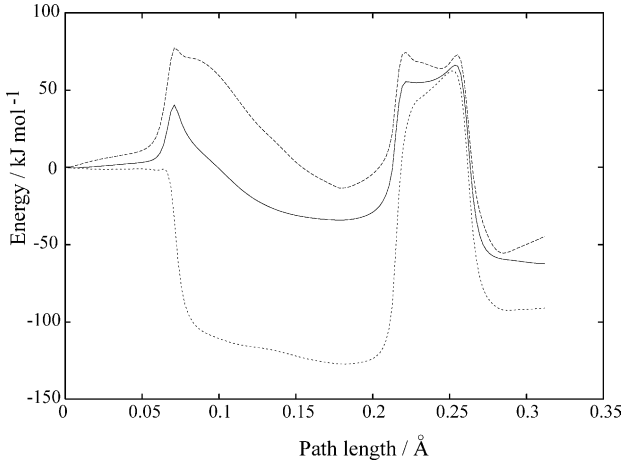

Fig. 8. Energy profile for mechanism 2 comparing the total energy barrier in the enzyme (solid line) with the energy of the QM region in vacuum (short-dashes). The sum of the QM and QM/MM electrostatic interaction energies in the enzyme is shown by the long-dashed line.

Fig. 8 shows that the reaction is more exergonic in vacuum, but that the barrier for the second step, which is rate limiting, is higher than in the enzyme (about 186 kJ mol^{-1}). In contrast, the proton transfer has no barrier. The

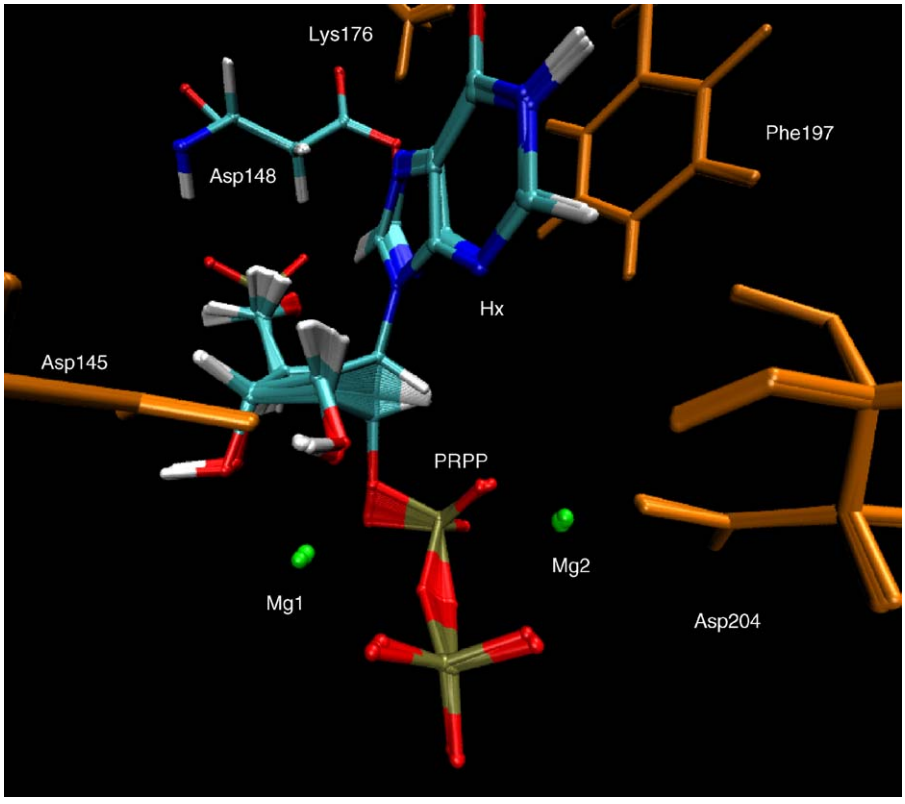

Fig. 7. Superposition of the NEB structures from the nucleophilic substitution step of mechanism 2. Clearly those atoms directly involved in the phosphoribosyl transfer show the most displacement. Asp148, hypoxanthine (Hx) and PRPP are shown in standard colours and some selected residues in orange.

explanation for this could be that the enzyme has been modelled by evolution to reduce the rate-limiting step, and this will be favoured even at the expense of increasing other, smaller barriers.

Also plotted in the figure is the contribution to the total energy in the enzyme coming from the sum of the QM and the QM/MM electrostatic interaction energies. This shows that the proton transfer step is the rate-limiting step without the stabilization provided by the MM and QM/MM Lennard–Jones energies. These latter energies also reduce the barrier for the phosphoribosyl transfer, but not as significantly.

4.2. Temperature-dependent reaction paths

The effect of temperature on a reaction process is most properly examined by determining free energies or by performing dynamical simulations. However, methods do exist for including thermal effects in an approximate way in reaction path calculations. One of these is based on the Smoluchowski equation which is a diffusion-like equation that includes forces due to a potential energy function [31,32]. This equation can be recast within a NEB formalism and allows the calculation of temperature-dependent paths [33]. Temperature tends to make optimal paths shorter, as can be seen when one considers that an optimal path would be a straight line at infinite temperature.

Calculation of such paths for the HGXPRTase reaction is straightforward and takes no more time than that with the standard NEB method. The paths at 312 K (human body temperature) for the same mechanisms detailed previously are shorter, but not remarkably so, because the diffusion contribution is small compared to the energy barriers and so the curvature of the path is not changed quantitatively. Due to the small differences between the 312 K and 0 K paths, we do not show any of them here.

5. Conclusions

In this article, we have discussed our implementation of the nudged elastic band method for finding minimum energy transition paths. We illustrated its use with an application to the reaction catalyzed by the enzyme, HGXPRTase, which we had studied previously using other theoretical approaches. We found two distinct stepwise mechanisms for the reaction in our NEB study although the lowest energy path corresponds to the favoured mechanism that we found in our earlier work.

In general, we consider that statistical-based approaches, such as free-energy calculations, are the methods of choice for fully understanding reactions in condensed phase systems. Nevertheless, the NEB method certainly has its place as a complement to other techniques and we intend to make routine use of it in our future studies of reaction mechanisms.

Acknowledgements

The authors would like to thank the Ramón y Cajal programme (RC), the Institut de Biologie Structurale – Jean-Pierre Ebel, the Commissariat à l'Energie Atomique (CEA) and the Centre National de la Recherche Scientifique (CNRS) for support of this work.

References

[1] H. Eyring, The activated complex in chemical reactions, J. Chem. Phys. 3 (1935) 107–115.
[2] H.B. Schlegel, Exploring potential energy surfaces for chemical reactions: an overview of some practical methods, J. Comput. Chem. 24 (2003) 1514–1527.
[3] R. Czerminski, R. Elber, Self-avoiding walk between two fixed points as a tool to calculate reaction paths in large molecular systems, Int. J. Quantum Chem.: Quantum Chem. Symp. 24 (1990) 167–186.
[4] G. Henkelman, G. Jóhannesson, H. Jónsson, Methods for finding saddle points and minimum energy paths, in: S.D. Schwartz (Ed.), Theoretical Methods in Condensed Phase Chemistry, Vol. 5, Progress on Theoretical Chemistry and Physics, Kluwer Academic Publishers, 2000, pp. 269–300.
[5] H. Jónsson, G. Mills, K.W. Jacobsen, Nudged elastic band method for finding minimum energy paths of transitions, in: B.J. Berne, G. Ciccotti, D.F. Coker (Eds.), Classical and quantum dynamics in condensed phase simulations, World Scientific, Singapore, 1998 , pp. 385–404.
[6] S.S.-L. Chiu, J.J.W.M. Douall, I.H. Hillier, Prediction of whole reaction paths for large molecular systems, J. Chem. Soc. Faraday Trans. 90 (1994) 1575–1579.
[7] M.J. Field, A practical introduction to the simulation of molecular systems, Cambridge University Press, Cambridge, UK, 1999.
[8] W.F. van Gunsteren, Methods for calculation of free energies and binding constants: successes and problems, in: W.F. van Gunsteren, P.K. Weiner (Eds.), Computer simulation of biomolecular systems: theoretical and experimental applications, ESCOM Science Publishers B.V., The Netherlands, 1989, pp. 27–59.
[9] A. Michalak, T. Ziegler, First-principle molecular dynamic simulations along the intrinsic reaction paths, J. Phys. Chem. A 105 (2001) 4333–4343.
[10] A. Thomas, M.J. Field, Reaction Mechanism of the HGXPRTase from *Plasmodium flaciparum*: a hybrid potential quantum mechanical/molecular mechanical study, J. Am. Chem. Soc. 124 (42) (2002) 12432–12438.
[11] W.D.L. Musick, Structural features of the phosphoribosyltransferases and their relationship to the human deficiency disorders of purine and pyrimidine metabolism, CRC Crit. Rev. Biochem. X (1981) 1–34.
[12] S.P. Craig, A.E. Eakin, Purine phosphoribosyltransferases III, J. Biol. Chem. 275 (2000) 20231–20234.
[13] M.J. Field, M. Albe, C. Bret, F. Proust-de Martin, A. Thomas, The Dynamo library for molecular simulations using hybrid quantum mechanical and molecular mechanical Potentials, J. Comput. Chem. 21 (2000) 1088–1100.
[14] P. Amara, M.J. Field, Combined quantum mechanical and molecular mechanical potentials, in: P. Kollman, N. Allinger (Eds.), Encyclopedia of Computational Chemistry, Wiley, 1998, pp. 179–183.
[15] P. Sherwood, Hybrid quantum mechanics/molecular mechanics approaches, in: Johannes Grotendorst, (Ed.), Modern Methods and Algorithms of Quantum Chemistry Proceedings, second ed., NIC series, John von Neumann Institute for Computing, Jülich, 2000. pp. 285–305.

[16] P.G. Bolhuis, C. Dellago, D. Chandler, Reaction coordinates of biomolecular isomerization, Proc. Natl. Acad. Sci. 97 (11) (2000) 5877–5882.
[17] J. Apostolakis, P. Ferrara, A. Caflisch, Calculation of conformational transitions and barriers in solvated systems: application to the alanine dipeptide in water, J. Chem. Phys. 110 (4) (1999) 2099–2108.
[18] W.L. Jorgensen, D.S. Maxwell, J. Tirado-Rives, Development and testing of the OPLS all-atom force field on conformational energetics and properties of organic liquids, J. Am. Chem. Soc. 118 (1996) 11225–11236.
[19] W. Shi, C.M. Li, P.C. Tyler, R.H. Furneaux, S.M. Cahill, M.E. Girvin, C. Grubmeyer, V.L. Schramm, S.C. Almo, The 2.0 Å structure of malarial purine phosphoribosyltransferase in complex with a transition-state analogue inhibitor, Biochemistry 38 (1999) 9872–9880.
[20] A. Heroux, E.L. White, L.J. Ross, A.P. Kuzin, D.W. Borhani, Substrate deformation in a hypoxanthine-guanine phosphoribosyltransferase ternary complex: the structural basis for catalysis, Struct. Fold Des. 8 (12) (2000) 1309–1318.
[21] M.J.S. Dewar, E.G. Zoebisch, E.F. Healy, J.J.P. Stewart, AM1: A new general purpose quantum mechanical molecular model, J. Am. Chem. Soc. 107 (1985) 3902–3909.
[22] S.A. Trygubenko, D.J. Wales, A doubly nudged elastic band method for finding transition states, J. Chem. Phys. 120 (2004) 2082–2094.
[23] J.-W. Chu, B.L. Trout, B. Brooks, A super-linear minimization scheme for the nudged elastic band method, J. Chem. Phys. 119 (24) (2003) 12708–12717.
[24] E. Weinan, W. Ren, E. Vanden-Eijnden, String method for the study of rare events, Phys. Rev. B 66 (2002) 052301.
[25] G. Henkelman, H. Jónsson, Improved tangent estimate in the nudged elastic band method for finding minimum energy paths and saddle points, J. Chem. Phys. 113 (2000) 9978–9985.
[26] B. Peters, A. Heyden, A.T. Bell, A. Chakraborty, A growing string method for determining transition states: comparison to the nudged elastic band and string methods, J. Chem. Phys. 120 (2004) 7877–7886.
[27] P. Maragakis, S.A. Andreev, Y. Brumer, D.R. Reichman, E. Kaxiras, Adaptive nudged elastic band approach for transition state calculation, J. Chem. Phys. 117 (10) (2002) 4651–4657.
[28] L. Xie, H. Liu, W. Yang, Adapting the nudged elastic band method for determining minimum energy paths of chemical reactions in enzymes, J. Chem. Phys. 120 (2004) 8039–8052.
[29] K. Müller, L.D. Brown, Location of saddle points and minimum energy paths by a constrained simplex optimization procedure, Theor. Chim. Acta 53 (1979) 75–93.
[30] V.L. Schramm, W. Shi, Atomic motion in enzymatic reaction coordinates, Curr. Op. Struct. Biol. 11 (2001) 657–665.
[31] M. Berkowitz, J.D. Morgan, J.D. McCammon, S.H. Northrup, Diffusion-controlled reactions: a variational formula for the optimum reaction coordinate, J. Chem. Phys. 79 (1983) 5563–5565.
[32] S. Huo, J.E. Straub, The Max Flux algorithm for calculating variationally optimized reaction paths for conformational transitions in many body systems at a finite temperature, J. Chem. Phys. 107 (1997) 5000–5006.
[33] R. Crehuet, M.J. Field, A temperature-dependent nudged-elastic-band algorithm, J. Chem. Phys. 118 (2003) 9563–9571.